Improving optical micromanipulation with force-feedback bilateral coupling

Edison Gerena, Florent Legendre, Youen Vitry, Stephane Regnier, Sinan Haliyo

Improving Optical Micromanipulation with Force-Feedback Bilateral Coupling

Edison Gerena[1], Florent Legendre[1], Youen Vitry[2], Stéphane Régnier[1] and Sinan Haliyo[1]

***Abstract*— Micromanipulation is challenging due to the specific physical effects governing the microworld. Interactive approaches using only visual feedback are limited to the 2D image of the microscope, and have forcibly lower bandwidth. Recently, haptic feedback teleoperation systems have been developed to try to overcome those difficulties. This paper explores the case of an optical tweezers platform coupled to an haptic device providing transparent force feedback. The impact of haptic feedback regarding user dexterity on tactile exploration tasks is studied using 3 µm microbeads and a test bench with micro sized shapes. The results reveal a consistent improvement in both users' trajectory tracking and their control of the contact forces. This also validates the experimental setup which performed reliably on 140 different trials of the evaluation.**

I. Introduction

Interactive micromanipulation has gained much attention due to a wide range novel of applications such as biological cell manipulation, drug delivery and microassembly. Among current techniques, Optical Tweezers (OT) is suitable for the manipulation of synthetic and biological samples ranging from a hundred of nanometres to tenth of millimeters, in a confined environment such a microfluidic devices.

Optical tweezers uses the pressure of light radiation to trap an object by providing a steep potential well in all axes, generated by the balance between the gradient forces on the optical plane (x,y) and the scattering force in the normal direction (z). This is usually obtained with a highly focused laser beam [1]. Controlling multiple focal spots enables to simultaneously trap and manipulate several objects in 3D [2], [3]. Optical manipulation has been applied to a large range of applications such as cell rotation [4], microassembly [5] and the actuation of microrobots [3].

Furthermore, optical forces on trapped spherical objects can be modelled linearly, as the restoring optical force is proportional to the distance from its equilibrium position. This particularity has led to the use of optical trapping for quantitative force measurements [6], such as the strength of inter-molecular bonds [7] or the stiffness of a cell membrane [8]. The optical trap acts as a spring with a stiffness proportional to the light intensity [9]. Well-established methods exist for precise stiffness calibration [10]. Hence, force sensing directly stems from the capability to track the position of the trapped object.

The position detection is commonly obtained through optical means, for example by a quadrant photodiode (QPD) [11] or digital cameras [12]. Photo-detection based techniques have high precision and high-bandwidth. However, they are not suitable for micromanipulations tasks, as they are very vulnerable to occlusions and environmental disturbances. Visual tracking algorithms using CMOS cameras offer straightforward implementations, but their bandwidth is limited by the amount of data that should be transmitted and processed. Real-time force information is hardly available. To overcome this issue, a tracking technique using an event-based camera is demonstrated [13], providing 3D force measurements in real-time.

Due to the difficulty to access the force sensing, there are only few works implementing a closed force control loop for optical manipulation. Most approaches are open-loop techniques [14], [15], [16], or automated one based on position [17], [18], [19]. However, in optical tweezers, objects are stably trapped up to a force threshold. This threshold is easily reached in most cases, for example by drag forces occurring during manipulation, ejecting the trapped object. Also, handling physical contact and interactions in terms of force is a key capability in robot control [20], [21]. Hence, force control approach implies immediate benefits in robotic optical tweezers.

Moreover, forces in the environment are important sources of information to complement the visual feedback and allow estimating physical characteristics such as stiffness or surface condition. As in macroscale, it is expected that user dexterity and precision would improve by enriching their perception. Consequently, several haptic-feedback teleoperated systems dedicated to micromanipulation have been proposed [22], [23]. Direct coupling between the macro and microenvironments arise several control issues [24]. High scaling factors (from picoNewton to Newton) amplify the signal noise and other measured signals as Brownian motion, reducing system stability and operator's understanding. Concerning optical manipulation, Arai et al. [25] have proposed the first haptic coupling for optical tweezers. 2D haptic explorations of microsurfaces have been demonstrated [26], [27]. 2D Multi-trap bilateral teleoperation of optical tweezers has also been proposed [28], [29]. Recently, a proof of concept of the first 3D haptic optical tweezers system was demonstrated [13].

These prototypes of haptic optical tweezers allow con-

*This work was supported by the French National Research Agency through the ANR-IOTA project (ANR-16-CE33-0002-01), and partially by the French government research program "Investissements d'avenir" through the Robotex Equipment of Excellence (ANR-10-EQPX-44).

[1]Authors are with Sorbonne Université, CNRS, Institut des Systèmes Intelligents et de Robotique, ISIR, F-75005 Paris, France.

[2]Y. Vitry is with Université libre de Bruxelles, BEAMS dpt, CP 165/56, 50 avenue Roosevelt, B-1050 Brussels.

(Correspondence e-mail: edison.gerena@isir.upmc.fr)

ducting micromanipulation tasks in a more flexible and intuitive way. However, in these works experiments are generally done by their creators, albeit potential end-users are not roboticians, but lab technicians who expect a turn-key system. Some works studied the usefulness of haptic feedbacks combined with optical tweezers. Lee et al. [30] proposed a model to simulate force interactions between a particle and a laser beam for haptic manipulation of microparticles, but their work is purely theoretical. Artificial guides and force-fields are explored to help the operator steer the trapped particle, avoiding collisions and contacts with other particles [31], [32], [33]. However, these experiments use virtual forces to improve the manipulation efficiency of optical tweezers systems. No study has evaluated a direct bilateral coupling with naive users.

We report here a systematic study on a bilaterally coupled haptic teleoperation on optical tweezers, providing real-time force sensing and straightforward human/machine interaction. We conduct haptic exploration experiments of microsynthetic objects with 14 subjects, resulting in 280 micromanipulation trials, comparing performances with and without force-feedback couplings. The use of synthetic objects helps the repeatability of the experiments and provides a ground truth for the shapes explored. The results indicate that haptic feedback improves the operator's dexterity in practical micromanipulation tasks, and improves by 35% the success rate in exploration tasks.

II. Methods

A. Haptic Optical Tweezers Platform

A versatile optical manipulation system (see Fig. 1) with 3D haptic feedback was designed to offer robust and intuitive control of suspended microbeads. Note that human sense of touch functions over a significant band of frequencies reaching 500 Hz. Double this value is considered a requirement for the control bandwidth to maintaining stability and a quality perception. The latency should not exceed 2 or 3 sampling periods [24]. This particular setup provides 3D high-speed and high resolution force sensor, deployed in hard real-time to guarantee 1 kHz control-loop frequency.

1) Optical Tweezers: The custom optical tweezers uses a 1064nm laser source (working power output : 300 mW). The laser source is directed into an oil immersion objective (Olympus UPlanFLN 40x, NA 1.3) creating a fixed optical trap in the focus plane. The sample-holder is mounted on redundant motion stages, hence controlling the 3D position of the sample-chamber in a large workspace, while the trapped object remains fixed in the optical plan. Two 2D microstages (PI, M126.CG) and a 3D motorized nanostage (PI, P562.3CD) are used for planar coarse positioning and x-y-z fine positioning respectively.

The illumination (LED, 3W) goes through the same objective and is divided by a beam splitter to two cameras: a conventional CMOS camera (Basler 659×494 px) and the asynchronous event-based image sensor (ATIS). The former

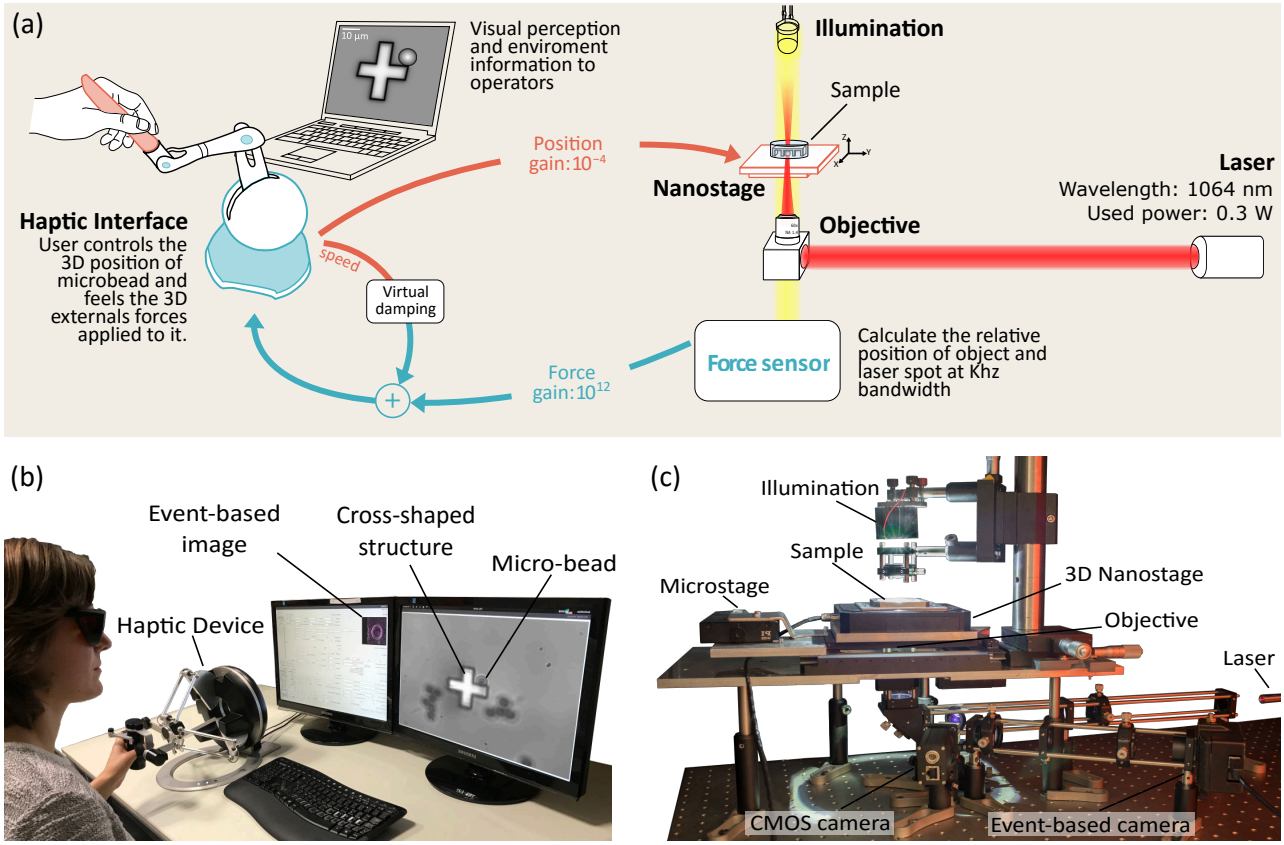

Fig. 1. (a) Schematic representation of the haptic optical tweezers platform. (b) Master device and user interface. (c) Slave device and optical path.

provides the environment and visual feedback to operators, while the latter is used to infer force information.

2) 3D High-speed Force Sensing: The force applied to the bead is computed using the optical force model [9] :

$$\mathbf{F}_{opt} = \mathbf{K} \times (\mathbf{P}_{laser} - \mathbf{P}_{bead}) \quad (1)$$

where $(\mathbf{P}_{laser} - \mathbf{P}_{bead})$ is the difference between the focus point of the optical trap and the bead position. $\mathbf{K}$ is the stiffness and was estimated experimentally using the Equipartition method [10] as K_x=12.3 pN/µm, K_y=12.6 pN/µm and K_z=1.5 pN/µm for 300 mW laser power.

The trapped bead's motion is measured using an event-based camera (ATIS from Prophesee, 240×304 px). In this sensor, each pixel responds asynchronously and independently to light intensity variations above a threshold, just like the spikes in human retina. Thereby, the system captures only the dynamic information and the amount of data to be processed is therefore considerably reduced, which makes it possible to process at speeds up to 10k fps [34]. A tracking algorithm is specially crafted for this sensor to extract the trapped objects' motion [13].

For a 3 µm microbead, the force detection range is 36.9, 37.8 and 4.5 pN for x, y and z respectively, with a planar theoretical resolution of 0.3 pN and an axial resolution of 0.25 pN. Please note that the Brownian motion's amplitude is approximately ten times higher than those resolution values for the given bead.

3) Bilateral Coupling: A direct bilateral coupling has been implemented, where the master position drives the trap position, and sensed forces are sent to the haptic device with linear scaling factors [24]. Although this approach gives the best transparency, the amplification of high-frequency noise degrades user perception. A dissipation block is hence inserted by virtually damping the force signal sent to the user. This is equivalent to a simple low-pass filter.

Users control the 3D position of the haptic interface (Omega.7, ForceDimension). Then, these translations are scaled down by $G_{p.xy} = 1.5\times10^{-4}$ and $G_{pz} = 0.9\times10^{-4}$ and sent to the nanostage to control the trap position relatively to sample holder. Finally, estimated forces are scaled up by $G_{f.xy} = 0.3\times10^{12}$ and $G_{fz} = 1.2\times10^{12}$ and send to the master device. The scaling factors in position is chosen as to cover 40×40×20 µm^3 in the optical tweezers workspace. Scaling factors in force are empirically chosen for a subjectively optimum tactile perception.

The entire solution is deployed on a hard real-time framework (co-kernel, Xenomai) to guarantee 1 kHz control-loop rate. The proposed direct coupling provides very good transparency as the force signal sent to the haptic device is a linear function of the sensor output. Fig. 3 depicts both these signals during a manipulation. A slight difference appears due to the virtual dissipation and the mechanical response of the haptic device.

B. Micro-chip Test bench

To evaluate the utility of haptic feedback in micromanipulation experiments and to ensure the repeatability of the task, a test bench has been manufactured. Fig. 2 shows this chip containing different basic shapes ranging in size from 7 µm to 14 µm.

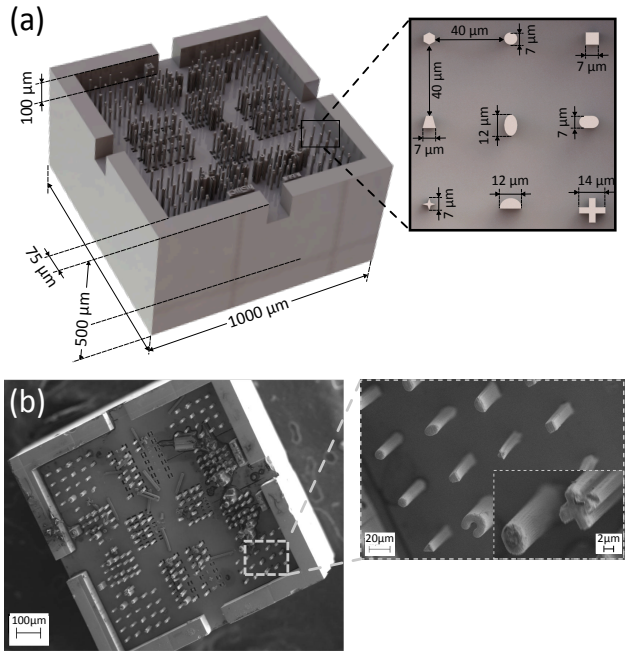

Fig. 2. (a) CAO model and dimensions of the the test bench microchip. (b) Scanning electron microscopy (SEM) image of the microchip.

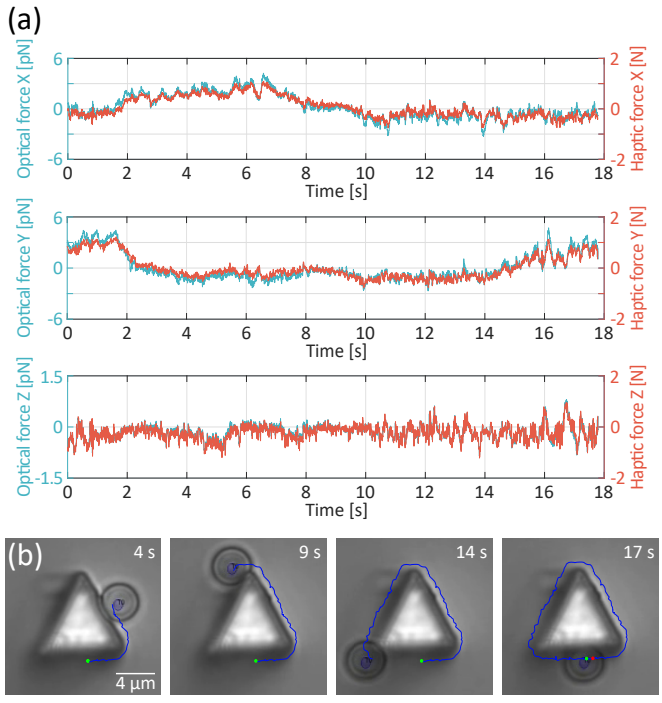

Fig. 3. Example of bilateral teleoperation in a triangle shape exploration task. (a) The 3D optical force applied on the microbead and the 3D haptic force feedback during the manipulation. (b) The 2D trajectory of the microbead during the triangle surface exploration.

The chip was printed using two-photon lithography with a Nanoscribe Photonic professional GT (Nanoscribe GmbH, Germany). The 63x objective and IP-Dip photoresist were used for printing to achieve the highest resolution (<1 µm) when writing 3D microstructure. After the completion of the printing, the wafer was submerged in PGMEA for 40 minutes and then in Isopropanol (IPA) for 30 minutes. After that, the IPA was removed by simply letting it evaporate in a clean room.

The entire chip body has been designed to the millimeter scale, so that it can be simply manipulated with forceps. During an exploration task, the chip is placed in a Petri dish filled with a solution composed of 90% distilled water, 5% ethanol and 5% *Tween20* to prevent surface adhesions. It is oriented in a way that the columns with the micrometer size shapes come into contact with the cover-slip. Then, the microbeads are added from a solution using a micropipette. After each trial, the chip is washed with distilled water and IPA until evaporation.

III. Experimental Protocol

The goal of the experiment is to analyse the performance of the subjects in an exploration task with and without haptic feedback.

A. Participant

The set of 14 volunteers were from Sorbonne Université. The age range were from 20 to 30 years old. The accepted volunteers were all right handed and did not present any physical abnormality.

B. Tasks performed

The task is to explore edges of different shapes using a optically trapped microbead of 3 µm diameter. The participant needed to first establish contact between the microbead and the explored shape, then follow the edges of the shape while maintaining contact until a complete tour around the shape is done. If for any reason the microbead is ejected from the optical trap, the task ends and is logged as 'failed'. The bead ejection can typically be caused by an abrupt movement or an excessive pressure on the explored shape.

The complete set of tasks contains two exploration attempts of five different shapes located on the microfluidic chip. The five shapes are a square, a trapeze, a triangle, a half-circle and a cross. Participants were divided in two groups of equal number. A first group of 7 participants performs first the set of tasks with only visual feedback (V), then the set of tasks with visual feedback and haptic feedback (V+H). A second group of 7 participants performs the set of tasks with visual feedback and haptic feedback (V+H) first, then the set of tasks with only visual feedback (V).

Consequently, each participant performs 10 exploration tasks with visual feedback (V) and 10 with dual feedback (V+H), therefore a total of 140 trials were performed for each condition.

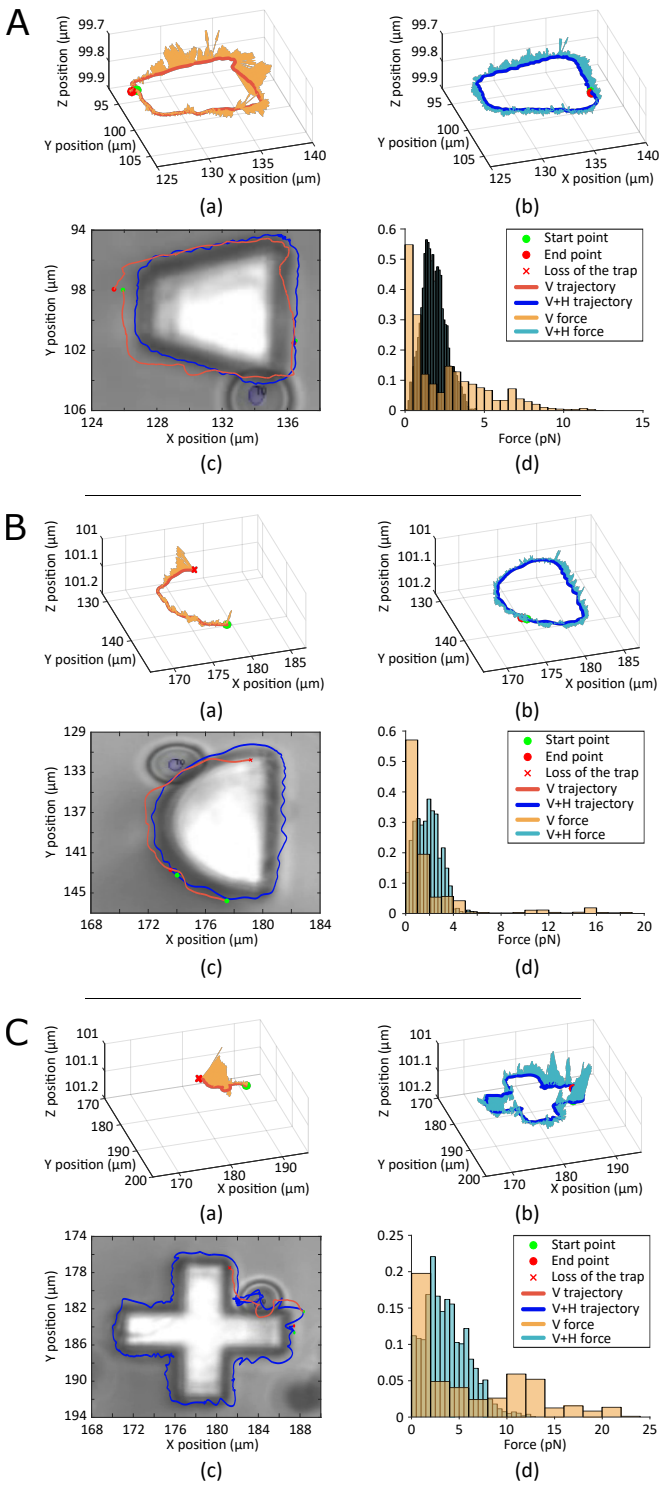

Fig. 4. Examples of an exploration of trapeze **(A)**, half-circle **(B)** and cross **(C)** shapes. (a) The 2D path of the microbead and the 3D contact forces during the experiment under vision condition (V). (b) The 2D path of the microbead and the 3D contact forces during the experiment under vision + haptic condition (V+H). (c) The trajectories of the microbead during the shapes surface exploration under the two conditions (V and V+H). (d) The histograms of the forces during the exploration task. Results are normalized to facilitate the comparison.

C. Conduct of the experiment

The experiments were conducted one participant at a time and each trial lasted around 30 minutes, depending on the participant's performance.

Before the formal evaluation, the participants were trained to use the system for 10 minutes and shown how to manipulate microbeads (3 μm, polystyrene) with the help of the haptic interface. An expert user traps a microbead, approaches the different shapes to explore, and constraints the z axis motion, then hands the control to the participant. This way the experiment is dissociated from the trapping phase and focuses on the feedback during execution.

IV. Results and Discussion

In order to evaluate the performances of the subjects, the position of the nanostage and the estimated force applied on the microbead are recorded at a rate of 500Hz during the complete duration of each task. After the experiments, the maximum, the mean and the standard deviation are extracted from the norms of the recorded forces for every task. Those force results are then used to compute the desired average maximum, average mean and average standard deviation displayed in Fig. 5, Fig. 6 and Fig. 7.

In addition, the task is written as failed if the participant loses the trapped microbead, and its data is used for the calculation of success rates shown in Fig. 5, Fig. 6 and Fig. 7.

Finally, the duration of each task is stored to evaluate the timing aspect of the participants performances.

A. Results per participant

Fig. 4 shows examples of exploration results in both condition (V) and (V+H) for the trapeze, the half-circle and the cross. Fig3.(a) and (b) show the path followed and the contact forces applied on the microbead during the contour exploration. Note that the forces are never completely null as a consequence of the Brownian motion applying constantly an erratic force on the bead, which is one of the important differences between macro-manipulation and micro-manipulation.

In A, the participant did not lose the microbead and complete the trapeze exploration task in both conditions (V) and (V+H). However, the representation of the forces shows a far more irregular pattern in condition (V) than in (V+H). The trajectory around the shape shown in Fig. 4.(c) reveals a more accurate tracking of the outline of the shapes when the haptic feedback is enabled. With vision only, the participant tends to move away from the shape or to apply excessive forces risking the loss of the microbead. In B and C , the participant loses the microbead in condition (V), but not in (V+H). A force spike can be seen near the end point when the bead was lost in (a) of B an C.

The distribution of the forces displayed in Fig. 4.(d) present a Gaussian shape in the condition (V+H), in contrast to the (V) case centered at 0pN with a decreasing slope. During the exploration in the condition (V+H), the participants exhibit a relatively constant force, relying obviously more on the haptic feedback than on vision for the fine movements. Without force information in the (V) condition, the participants were trying to interpret the visual feedback to evaluate the force applied, resulting in a more demanding situation hence less accurate movements. In the condition (V+H), the haptic information naturally integrates with the vision to achieve finer motor-control.

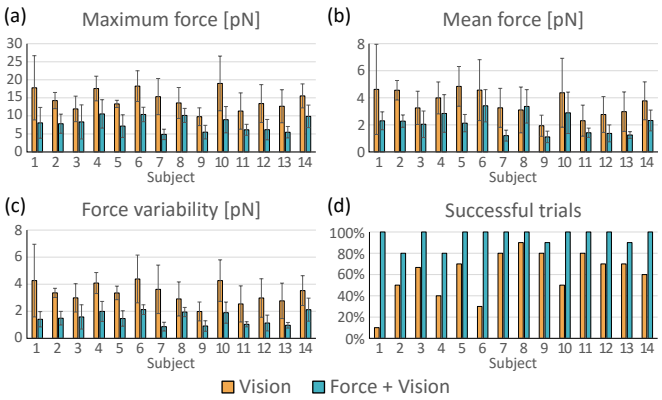

Fig. 5. Statistical results of the experiment per subject.

Fig. 5 depicts the force analysis and success rate for an individual subject. The most obvious result is the low rate of failed trials when haptic is used, as shown in Fig. 5.(d). It is effectively quite difficult to visually evaluate when the microbead risks to be ejected. The force feedback marks the difference by providing this critical information. The effect is also visible in the maximum force graph in Fig. 5.(a) which shows a decrease of the maximum force exerted, meaning that the participant manages the contact better, releasing pressure on the explored object when needed.

We also observe for 13 out of 14 participants a decrease in the mean force exerted between (V) and (V+H) (Fig. 5), attesting that participants proceed more gently when the haptic feedback is enabled.

The force variability shown in Fig. 5.(c) has dropped for every subject between (V) and (V+H), reflecting the previous observation on the force's distribution displayed in Fig. 4.(d). The participants naturally attempt to keep a constant force during the exploration in condition (V+H), which diminish the variability of the exerted forces.

No meaningful differences are observed in the individual results between the group starting with (V) and the group starting with (V+H). This absence of dissimilarity tends to demonstrate that no additional training is necessary to handle the haptic feedback. If a period of familiarization were needed, the participant starting with (V) would have performed better in (V+H) than the participant starting directly with (V+H) because they would have already completed 10 exploration tasks and substantially progressed in optical-manipulation.

B. Results per shape

Fig. 6 shows the average duration of the completed tasks and the corresponding success rate per shape. Only

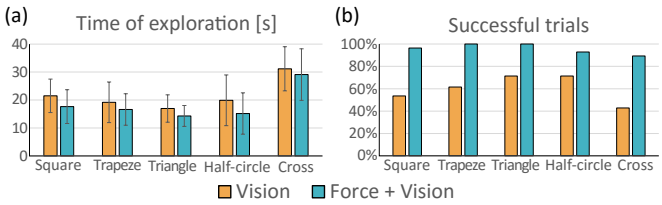

Fig. 6. Statistical results of the experiment for each shape.

successful trials are counted in the computation of the time of exploration.

A small decrease of duration is observed for each shape between (V) and (V+H). Since no instructions were given to go fast, it indicates that the participants tend to naturally proceed slightly better with the haptic feedback in condition (V+H). An expected inverse correlation appears between the duration of the task and the success rate. The most complex shape is the cross by the number of sharp corners. It has a longer duration of exploration and a lower successful trial rate, while a simpler shape like the triangle shows shorter duration of exploration and a higher success rate.

C. General results

In Fig. 7 are displayed global results representing the average data of all participants over all shapes. Between (V) and (V+H), the average maximum force decreases by 46.0% (6.70pN) and the average force drops by 40.4% (1.45pN). The force variability drops by 55.7% (1.87pN). Finally, the global successful trials rate rises by 35% from 61% to 96%, meaning that the fail rate is divided by almost 10 from 39% in (V) to 4% in (V+H).

To perform optical-micromanipulations, visual feedbacks are suffering from two major issues. First, the broadcasted image is a 2D projection of a 3D workspace. The operator faces difficulties to apprehend the working environment and a mental effort is required to grasp a clear 3D representation of the ongoing manipulation. Secondly, an objective with high numerical aperture is necessary to create an optical tweezer. The focused region of the resulting image is narrow and generates visual artefacts around the observed micro-structures. Those two aspects compromise the user's vision and thus his performances. In addition, the forces generated by an optical tweezer are weak and a trapped micro-object can easily be ejected by a collision or an abrupt movement.

The deployed haptic feedback system complements the visual feedback with 3D forces information. Therefore, it helps in the 3D apprehension of the workspace and in the perception of the forces exerted by the optical tweezer on the trapped microbead.

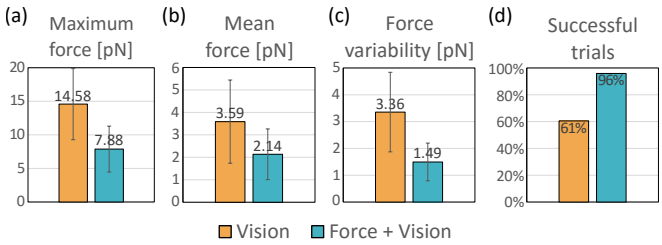

Fig. 7. Statistical global results of the experiment.

V. Conclusion

This study demonstrates that haptic feedback improves the user performance in optical manipulation by a significant margin. Vision provides general overview information on the scene and haptic feedback is used for fine control when contacting or manipulating an object. The operator naturally integrates this additional information channel. Participants apply in average less pressure on the manipulated objects, their handling is smoother and contact forces exhibit far less variance. The decrease in the execution duration let also assume a better mental efficiency, correlated to a lesser cognitive load, which indicates that the user considers the task easier [35], [36].

Therefore, proposed multimodal stimuli enables users to better apprehend microscale phenomenons and be more effective to achieve desired results during manipulation tasks.

Additionally, the 3D force complements the 2D vision information delivered by the microscope and allows users to react faster, as human haptic perception bandwidth is one order of magnitude higher than vision. This also gives a far richer information: for example changes in high-frequencies of the Brownian motion which would go unnoticed for the eyes becomes perceivable with haptics.

As an additional last remark, the system used in experiments also proved itself repeatable and reliable. The coupling is highly transparent, and no instability occurred on any of the 140 trials.

References

[1] A. Ashkin, J. M. Dziedzic, J. Bjorkholm, and S. Chu, "Observation of a single-beam gradient force optical trap for dielectric particles," *Optics letters*, vol. 11, no. 5, pp. 288–290, 1986.

[2] J. E. Curtis, B. A. Koss, and D. G. Grier, "Dynamic holographic optical tweezers," *Optics communications*, vol. 207, no. 1-6, pp. 169–175, 2002.

[3] E. Gerena, S. Regnier, and D. S. Haliyo, "High-bandwidth 3d multi-trap actuation technique for 6-dof real-time control of optical robots," *IEEE Robotics and Automation Letters*, 2019.

[4] M. Xie, A. Shakoor, Y. Shen, J. K. Mills, and D. Sun, "Out-of-plane rotation control of biological cells with a robot-tweezers manipulation system for orientation-based cell surgery," *IEEE Transactions on Biomedical Engineering*, 2018.

[5] J. Köhler, S. I. Ksouri, C. Esen, and A. Ostendorf, "Optical screw-wrench for microassembly," *Microsystems & Nanoengineering*, vol. 3, p. 16083, 2017.

[6] H. Zhang and K.-K. Liu, "Optical tweezers for single cells," *Journal of The Royal Society Interface*, vol. 5, no. 24, pp. 671–690, 2008.

[7] A. L. Stout, "Detection and characterization of individual intermolecular bonds using optical tweezers," *Biophysical journal*, vol. 80, no. 6, pp. 2976–2986, 2001.

[8] D. Raucher and M. P. Sheetz, "Characteristics of a membrane reservoir buffering membrane tension," *Biophysical journal*, vol. 77, no. 4, pp. 1992–2002, 1999.

[9] A. Ashkin, "Forces of a single-beam gradient laser trap on a dielectric sphere in the ray optics regime," *Biophysical journal*, vol. 61, no. 2, p. 569, 1992.

[10] K. C. Neuman and S. M. Block, "Optical trapping," *Review of scientific instruments*, vol. 75, no. 9, pp. 2787–2809, 2004.

[11] D. Ruh, B. Tränkle, and A. Rohrbach, "Fast parallel interferometric 3d tracking of numerous optically trapped particles and their hydrodynamic interaction," *Optics express*, vol. 19, no. 22, pp. 21 627–21 642, 2011.

[12] A. Huhle, D. Klaue, H. Brutzer, P. Daldrop, S. Joo, O. Otto, U. F. Keyser, and R. Seidel, "Camera-based three-dimensional real-time particle tracking at khz rates and ångström accuracy," *Nature communications*, vol. 6, 2015.

[13] M. Yin, E. Gerena, C. Pacoret, S. Haliyo, and S. Régnier, "High-bandwidth 3d force feedback optical tweezers for interactive biomanipulation," in *Intelligent Robots and Systems (IROS), 2017 IEEE/RSJ International Conference on*. IEEE, 2017, pp. 1889–1894.

[14] K. Onda and F. Arai, "Parallel teleoperation of holographic optical tweezers using multi-touch user interface," in *Robotics and Automation (ICRA), 2012 IEEE International Conference on*. IEEE, 2012, pp. 1069–1074.

[15] C. Muhiddin, D. Phillips, M. Miles, L. Picco, and D. Carberry, "Kinect 4 : holographic optical tweezers," *Journal of Optics*, vol. 15, no. 7, p. 075302, 2013.

[16] Z. Tomori, P. Keša, M. Nikorovič, J. Kaňka, P. Jákl, M. Šerỳ, S. Bernatová, E. Valušová, M. Antalík, and P. Zemánek, "Holographic raman tweezers controlled by multi-modal natural user interface," *Journal of Optics*, vol. 18, no. 1, p. 015602, 2015.

[17] S. Hu, H. Xie, T. Wei, S. Chen, and D. Sun, "Automated indirect transportation of biological cells with optical tweezers and a 3d printed microtool," *Applied Sciences*, vol. 9, no. 14, p. 2883, 2019.

[18] C. C. Cheah, Q. M. Ta, and R. Haghighi, "Grasping and manipulation of a micro-particle using multiple optical traps," *Automatica*, vol. 68, pp. 216–227, 2016.

[19] S. Chowdhury, A. Thakur, P. Svec, C. Wang, W. Losert, and S. K. Gupta, "Automated manipulation of biological cells using gripper formations controlled by optical tweezers," *IEEE Transactions on Automation Science and Engineering*, vol. 11, no. 2, pp. 338–347, 2014.

[20] D. E. Whitney, "Historical perspective and state of the art in robot force control," *Proceedings. 1985 IEEE International Conference on Robotics and Automation*, vol. 2, pp. 262–268, 1985.

[21] B. Siciliano and L. Villani, *Robot force control*. Springer Science & Business Media, 2012, vol. 540.

[22] A. Bolopion and S. Régnier, "A review of haptic feedback teleoperation systems for micromanipulation and microassembly," *IEEE Transactions on automation science and engineering*, vol. 10, no. 3, pp. 496–502, 2013.

[23] C. Pacchierotti, S. Scheggi, D. Prattichizzo, and S. Misra, "Haptic feedback for microrobotics applications: A review," *Frontiers in Robotics and AI*, vol. 3, p. 53, 2016.

[24] A. Bolopion, B. Cagneau, D. S. Haliyo, and S. Régnier, "Analysis of stability and transparency for nanoscale force feedback in bilateral coupling," *Journal of Micro-Nano Mechatronics*, vol. 4, no. 4, p. 145, 2008.

[25] F. Arai, M. Ogawa, and T. Fukuda, "Indirect manipulation and bilateral control of the microbe by the laser manipulated microtools," in *Proceedings. 2000 IEEE/RSJ International Conference on Intelligent Robots and Systems (IROS 2000)(Cat. No. 00CH37113)*, vol. 1. IEEE, 2000, pp. 665–670.

[26] C. Pacoret, R. Bowman, G. Gibson, S. Haliyo, D. Carberry, A. Bergander, S. Régnier, and M. Padgett, "Touching the microworld with force-feedback optical tweezers," *Optics express*, vol. 17, no. 12, pp. 10 259–10 264, 2009.

[27] Z. Ni, C. Pacoret, R. Benosman, and S. Régnier, "2d high speed force feedback teleoperation of optical tweezers," in *Robotics and Automation (ICRA), 2013 IEEE International Conference on*. IEEE, 2013, pp. 1700–1705.

[28] K. Onda and F.Arai, "Multi-beam bilateral teleoperation of holographic optical tweezers," *Opt. Express*, vol. 20, no. 4, pp. 3633–3641, Feb 2012.

[29] Z. Ni, M. Yin, C. Pacoret, R. Benosman, and S. Régnier, "First high speed simultaneous force feedback for multi-trap optical tweezers," in *2014 IEEE/ASME International Conference on Advanced Intelligent Mechatronics*. IEEE, 2014, pp. 7–12.

[30] L. Lee, Lyons, "Virtual environment for manipulating microscopic particles with optical tweezers," *Journal of research of the National Institute of Standards and Technology*, vol. 108, no. 4, pp. 275–287, 2003.

[31] C. Basdogan, A. Kiraz, I. Bukusoglu, A. Varol, and S. Doğanay, "Haptic guidance for improved task performance in steering microparticles with optical tweezers," *Optics Express*, vol. 15, no. 18, pp. 11 616–11 621, 2007.

[32] I. Bukusoglu, C. Basdogan, A. Kiraz, and A. Kurt, "Haptic manipulation of microspheres using optical tweezers under the guidance of artificial force fields," *Presence: Teleoperators and Virtual Environments*, vol. 17, no. 4, pp. 344–364, 2008.

[33] M. Grammatikopoulou and G.-Z. Yang, "Gaze contingent control for optical micromanipulation," in *Robotics and Automation (ICRA), 2017 IEEE International Conference on*. IEEE, 2017, pp. 5989–5995.

[34] X. Lagorce, C. Meyer, S.-H. Ieng, D. Filliat, and R. Benosman, "Asynchronous event-based multikernel algorithm for high-speed visual features tracking," *IEEE transactions on neural networks and learning systems*, vol. 26, no. 8, pp. 1710–1720, 2014.

[35] F. Paas, P. Ayres, and M. Pachman, *Assessment of Cognitive Load in Multimedia Learning Theory, Methods and Applications*, 11 2008, pp. 11–35.

[36] F. A. Haji, D. Rojas, R. Childs, S. de Ribaupierre, and A. Dubrowski, "Measuring cognitive load: performance, mental effort and simulation task complexity," *Medical Education*, vol. 49, no. 8, pp. 815–827, 2015. [Online]. Available: https://onlinelibrary.wiley.com/doi/abs/10.1111/medu.12773